AIP Advances

Cone angle effects on noise characteristics of jets impinging on conical obstacles

Cite as: AIP Advances **8**, 115121 (2018); https://doi.org/10.1063/1.5051484
Submitted: 09 August 2018 • Accepted: 07 November 2018 • Published Online: 19 November 2018

Xin Liu, Jun-long Xie, Qing Xie, et al.

View Online Export Citation CrossMark

ARTICLES YOU MAY BE INTERESTED IN

Effect of impingement surface roughness on the noise from impinging jets
Physics of Fluids **26**, 036101 (2014); https://doi.org/10.1063/1.4866977

An experimental investigation of a square supersonic jet and impinging jet on an inclined plate
AIP Advances **10**, 105132 (2020); https://doi.org/10.1063/5.0018727

The connection between sound production and jet structure of the supersonic impinging jet
The Journal of the Acoustical Society of America **111**, 735 (2002); https://doi.org/10.1121/1.1436069

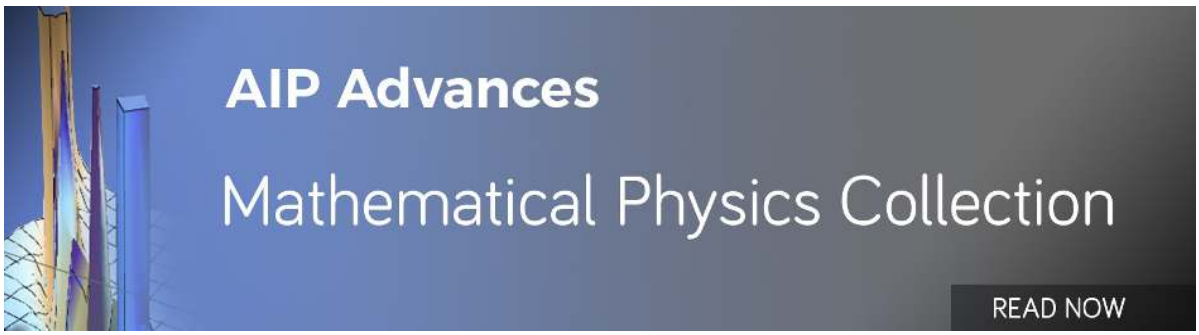

AIP Publishing

© 2018 Author(s).

Cone angle effects on noise characteristics of jets impinging on conical obstacles

Xin Liu, Jun-long Xie,[a] Qing Xie, and He-yuan Huang
School of Energy and Power Engineering, Huazhong University of Science & Technology, Wuhan 430074, China

(Received 9 August 2018; accepted 7 November 2018; published online 19 November 2018)

This paper presents an acoustic measurement experiment to investigate noise characteristics of jets impinging on conical obstacles of different cone angles. Besides cone angle, effects of impinging velocity and impinging distance are also studied. Overall sound pressure level (OASPL) and noise spectrum are analyzed. The results suggest that effects of cone angle on noise characteristics of the impinging jet are mainly related to the impinging distance. The main spectrum characteristic for impinging jet cases is of broadband characteristic in the middle and high frequency bands. Further, compared to the free jet case, main acoustic sources of the impinging jet for three cone angle cases are discussed under different impinging distances, combined with flow field analysis and spectrum analysis. Finally, a detailed noise directivity study is carried out. The OASPL of impinging jet for different cone angle cases is presented under various impinging distances and monitoring point positions. © *2018 Author(s). All article content, except where otherwise noted, is licensed under a Creative Commons Attribution (CC BY) license (http://creativecommons.org/licenses/by/4.0/).*
https://doi.org/10.1063/1.5051484

I. INTRODUCTION

Impinging jets are widely applied in many engineering and practical problems such as heating and cooling in industrial process, drying of textile and paper, preparation of transistors, and the take-off of rockets and aircrafts.[1] Study of the noise generated by these impinging jets has received great interest from researchers. In the last two decades, a large list of studies are about the noise characteristics and source mechanics of a supersonic jet impinging on the plate. Dhamanekar[2] experimentally investigated the noise characteristics of jets impinging on inclined plates of various surface roughness values. He found that the noise of a rough plate is less than that of a smooth plate when the high-speed jet impinging on the plates. Sinibaldi[3] carried out an experimental analysis of impinging surface effect on screech tones. The experimental results validated the coupling between acoustic discrete tones and mean and fluctuating flow velocities. Arthurs[4] investigated the tone generation of a high-speed jet impinging on a flat plate by experiment. Akamine[5] investigated the effect of nozzle-plate distance on the difference in the broadband acoustic field from a supersonic jet impinging on an inclined plate. Frendi[6] numerically studied the flow structures and the resulting noise from a supersonic impinging jet on a flat plate.

As the development of computer technology, numerical method is also widely applied. Romain[7] numerically investigated the tone generation in an expanded supersonic jet impinging on a flat plate by large-eddy simulation. Christoph et al.[8] focused on the noise generation mechanisms of a supersonic jet impinging on an inclined plate using large eddy simulation. Lyrintzis[9] numerically studied the acoustic field of a supersonic jet impinging on a flat plate. He showed the influence of the inclination angle on sound pressure level spectrum and noise directivity of the impinging jet. Yao et al.[10] suggested the interaction of shocks and vortices in a supersonic jet impinging on a flat plate

[a]Email of corresponding author: hustxjl@163.com

 © Author(s) 2018

using the large eddy simulation. Uzun[11] numerically investigated the interaction of the impinging jet with the flat impingement plate and provided the noise characteristics caused by the interaction. Nonomura[12] numerically studied the effects of plate angle on acoustic waves for a supersonic jet impinging on an inclined flat plate at various angles. Kim[13] focused on effects of the impinging distance and nozzle pressure ratio on the oscillatory flow features of a jet impinging on a flat plate.

In contrast, the research on the noise characteristics of low-speed impinging jet is relatively few. Powell[14,15] investigated the feedback mechanism for the generation of classical tonal noise and characteristics of noise sources in a low-speed impinging jet. Vinoth[16] examined the effect of the plate geometry on the self-excitation process of subsonic impinging jets on flat plates. Ren[17] investigated a vortex ring impinging on a circular cylinder using large eddy simulation. Moreover, the low-speed impinging jet is widely used in the industry of impingement cooling. Most researches focus on the heat transfer characteristics of impinging jet,[18–20] but ignoring the noise characteristics. The motivation for this paper is to experimentally investigate the acoustic characteristics of low-speed jets impinging on conical obstacles of different cone angles. The paper outline is as following. Section II details the experimental setup of noise measurement and velocity measurement used in this paper. Section III analyses the effects of impinging distance and cone angle on the flow field, overall sound pressure level (OASPL), mechanism of acoustic source and noise directivity. Finally, a summary of main findings is presented in Section IV.

II. EXPERIMENTAL SETUP AND PROCEDURE

A. Noise measurement

The noise measurement experiment is carried out to investigate the cone angle effects on noise characteristics and distribution of jets impinging on conical obstacles. The experimental setup for noise measurement is presented in Fig. 1. It consists of the low-Mach-number jet device, the control room and the anechoic chamber of size 3.5m × 3.5m × 3m (wedge tip-to tip). In order to reduce the influence of jet device on noise measurement, only the jet apparatus is arranged in the anechoic chamber and the metallic surfaces of the jet apparatus are covered with sound-absorbing cotton. The inner diameter of the nozzle outlet (D) is 10mm. The distance from the center of nozzle outlet to the ground is 1.79m. The velocity of nozzle outlet (impinging velocity) is varied from 20m/s to 60m/s in steps of 10m/s. The distance from the nozzle outlet to the conical obstacle (X) is equal to 10mm, 20mm, 50mm, 100mm and 200mm (X/D=1, 2, 5, 10 and 20), respectively. Conical obstacles have a fixed height with h=14mm, and different bottom diameters with d= 16mm (cone angle α=60°), 28mm (cone angle α=90°) and 48mm (cone angle α=120°). The material of these cones is aluminium alloy and the height of cone support is adjustable.

Noise monitoring points are arranged on a circular arc with R=1m as shown in Fig. 2. θ is the monitoring angle between central axis and the straight line from monitoring point to the center of nozzle outlet. There are 11 monitoring points in the range of 15° to 165° in intervals of 15°. 90° direction is perpendicular to the jet direction. The microphone sensor is PCB 377B11 with PCB 426E01. Data acquisitions are carried out with NI PXI-1042Q, PXI-4472 and PXI-8106 control system, which has a band width from 20Hz to 20 kHz. The sampling frequency is 48 kHz. The background sound pressure level is 19.9dB. Using above method, overall sound pressure level and noise spectrum of the impinging jet on different conical obstacles are measured under various monitoring positions, impinging velocities and impinging distances.

B. Velocity measurement

Velocity measurement experiment is performed to investigate the influence of cone angles on the flow field of jets impinging on the conical obstacle. As typical examples for comparison in the experiment, we choose the free jet case and the impinging jet cases with the impinging distance of 10mm and 100mm (X/D=1, 10). For the free jet case, velocity monitoring points are arranged in the central axis. The distance from monitoring point to the center of nozzle outlet is donated as X1. As for the impinging jet case, velocity monitoring points are arranged in two segments A and B, as shown in Fig. 3. Both A and B are in the central axis. A is in front of obstacle. The distance from A to the

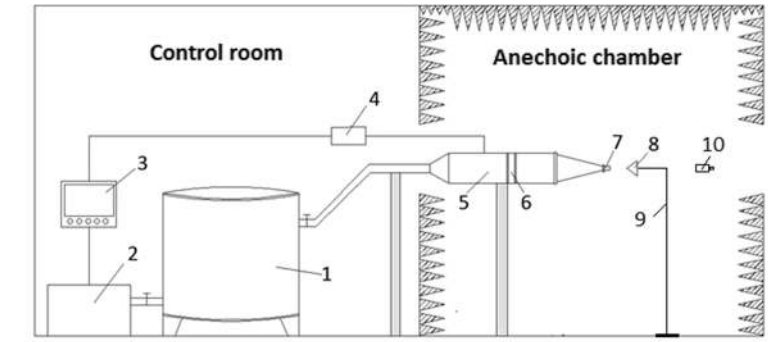

1-Gas tank 2-Compressor 3-PID controller 4-Differential pressure sensor 5-Diffuser section
6-Rectification section 7-Jet nozzle 8-Conical obstacle 9-Cone support 10-Microphone

(a)

(b)

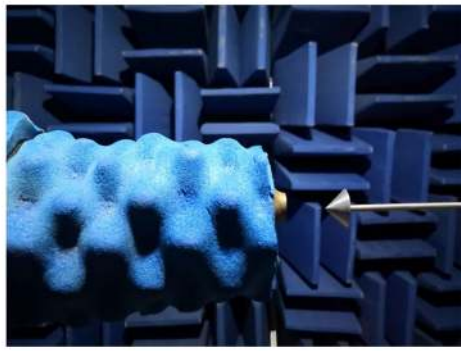

(c)

FIG. 1. Experimental setup for noise measurement. (a) Schematic view of experimental setup. (b) Low-Mach-number jet device. (c) Noise measurement room.

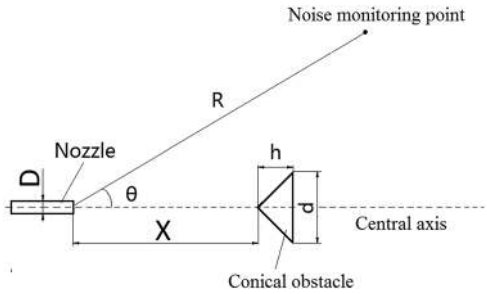

FIG. 2. Arrangement of noise monitoring points.

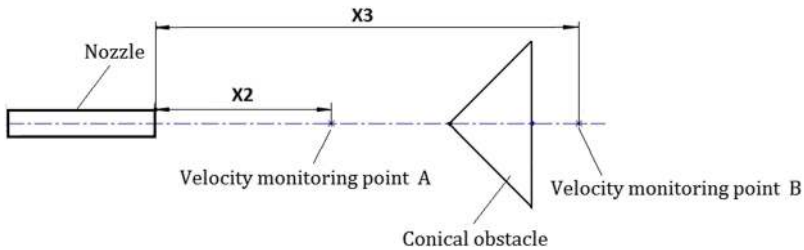

FIG. 3. Arrangement of velocity monitoring points for impinging jet cases.

center of nozzle outlet is donated as X2. B is behind the obstacle. The distance from B to the center of nozzle outlet is donated as X3. The impinging velocity is 60m/s. The velocity of monitoring point is obtained by the hot wire anemometer TESTO 416. The measuring precision of the instrument is ±2%. Using above method, velocity distribution along central axis in free jet case and impinging jet case of different cone angles is measured.

III. RESULTS AND DISCUSSION

A. Flow field analysis

Fig. 4 shows the velocity distribution along central axis in the free jet case. It can be seen that there is the potential core region in which the fluid keeps the initial velocity (60m/s). The length of the potential core region is about 60mm (6D). Then the velocity decreases rapidly. When X1 is larger than 100mm (10D), the trend of velocity attenuation gradually decreases with the development of the free jet.

Fig. 5 shows the schematic of the flow field for impinging jet case. The flow field of jet impinging on the conical obstacle consists of four regions: free jet region, stagnation flow region, wall jet region and downstream jet region. Combined with velocity distribution along central axis in impinging jet case as shown in Fig. 6, cone angle effects on the flow field of the jet impinging on the conical obstacle are analyzed. In the free jet region, the potential core area exists in three cone angle cases and the length of potential core area is almost the same for X=10D, however, the potential core area is seriously damaged for X=1D. The velocity for α=60° is larger than that for α=120° with the development of jet. In the stagnation flow region, the fluid impinges on the surface of the obstacle and the velocity decreases sharply. The attenuation rate of velocity for α=60° is much smaller than that in the other two cases. The attenuation rate of velocity for

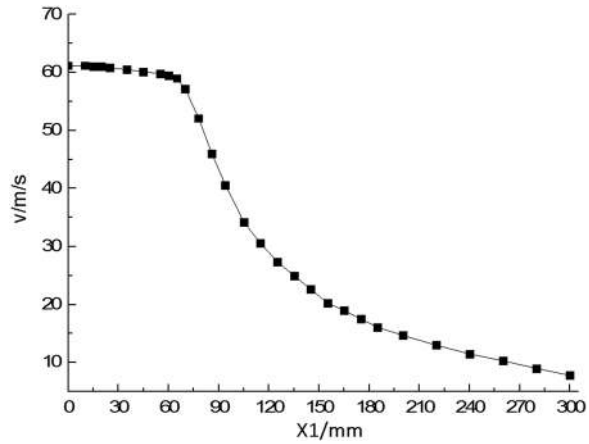

FIG. 4. Velocity distribution along central axis in free jet case.

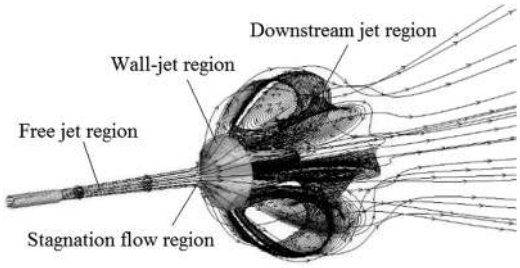

FIG. 5. Schematic of the flow field of impinging jet case.

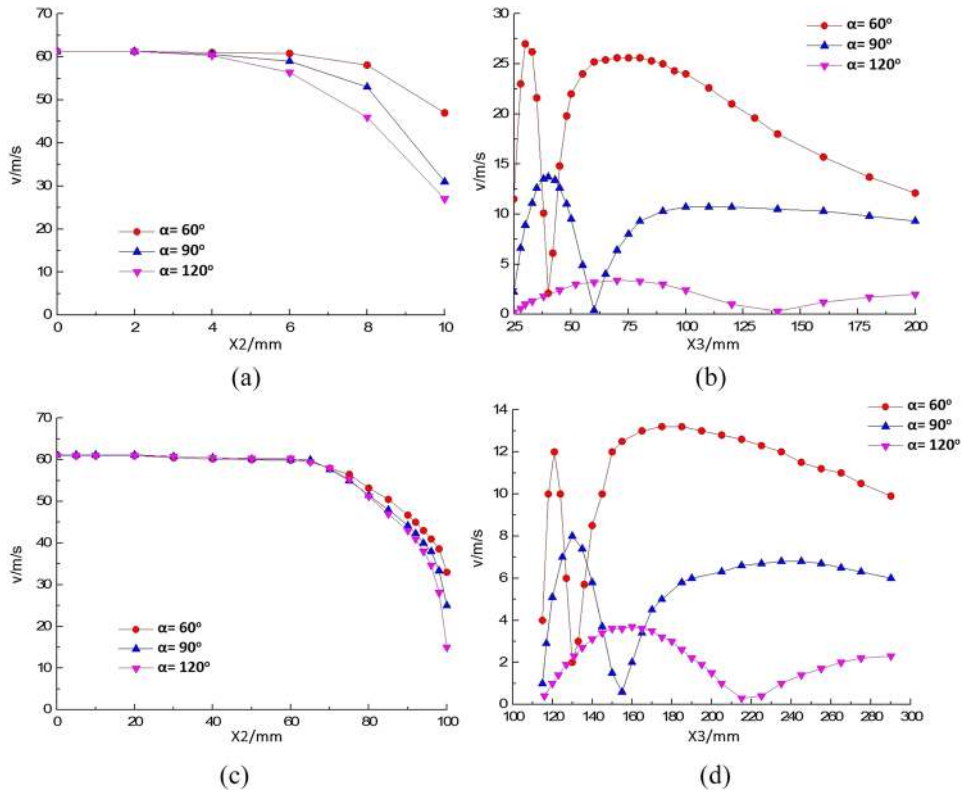

FIG. 6. Velocity distribution along central axis in impinging jet case at X/D=1 and X/D=10. (a) Velocity monitoring point A (X/D=1). (b) Velocity monitoring point B (X/D=1). (c) Velocity monitoring point A (X/D=10). (d) Velocity monitoring point B (X/D=10).

α=120° is the largest. In the wall jet region, the fluid flows to the surrounding area along the cone surface.

As for the downstream jet region, there are recirculation zones forming on the back of the cone after the vortices shedding from the cone. The trend of velocity distribution along the central axis is a wave line and the first peak value of velocity occurs in the cross area of the recirculation zones. According to the location and velocity magnitude of the peak velocity point, it can be inferred that for α=60°, the dimension of recirculation zone is the smallest and the intensity of circulating is the largest. As the cone angle increases, the dimension of recirculation zone increases, whereas the intensity of circulating decreases. In addition, for the same angle case, as the impinging distance increases, the intensity of circulating is reduced.

B. Overall sound pressure level

In order to effectively investigate the variation of acoustic characteristics with cone angle, overall sound pressure level (OASPL) of jets impinging on the conical obstacles of different cone angles is measured at various impinging distances and impinging velocities. Fig. 7 shows the variation of OASPL with impinging velocity for different cone angles. It can be observed that OASPL increases as the impinging velocity increases for all cone angles at different impinging distances. Then on, the cone angle has different effects depending on the impinging distance. For X=1D, OASPL is minimum with α=120°. As the cone angle decreases, OASPL first increases and then decreases. For X=5D, the OASPL with α=120° is similar to that with α=90°. The OASPL is minimum for α=60°. As for X=10D, the decrease of cone angle causes a decrease in OASPL.

In order to investigate the effect of impinging distance in detail, variation of OASPL with impinging distance for different cone angles is measured at θ=45°. The same experiments are repeated for

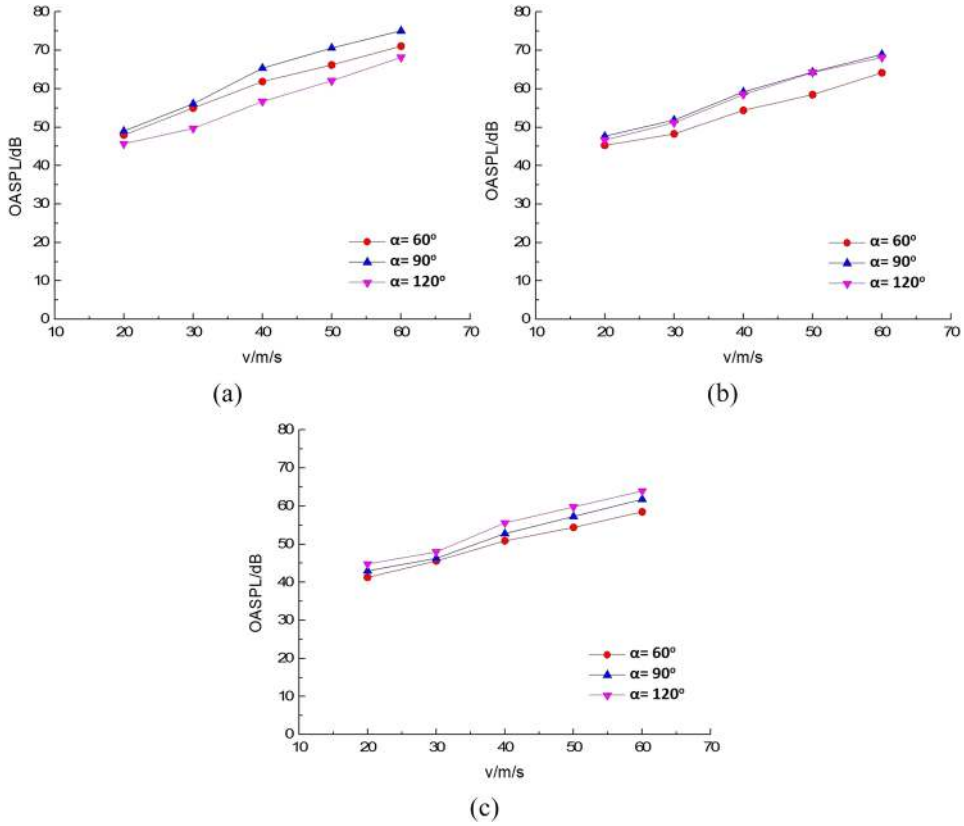

FIG. 7. Variation of OASPL with impinging velocity for different cone angles (θ=45°). (a) X=1D. (b) X=5D. (c) X=10D.

the free jet (without conical obstacle). As shown in Fig. 8, for all cone angle cases, the variation of OASPL under the impinging velocity of 30m/s is similar to that under the impinging velocity of 60m/s. OASPL of impinging jet is larger than that of the free jet. For α=60°, OASPL decreases with the increase of the impinging distance. However, as the cone angle increases, the effect of the impinging distance is not the same. As the impinging distance increases, the OASPL first increases and then decreases with α=90° and 120°. The maximum value occurs at X=2D. In addition, for all cone angle cases, the increase of impinging distance causes a decrease in OASPL when X>5D.

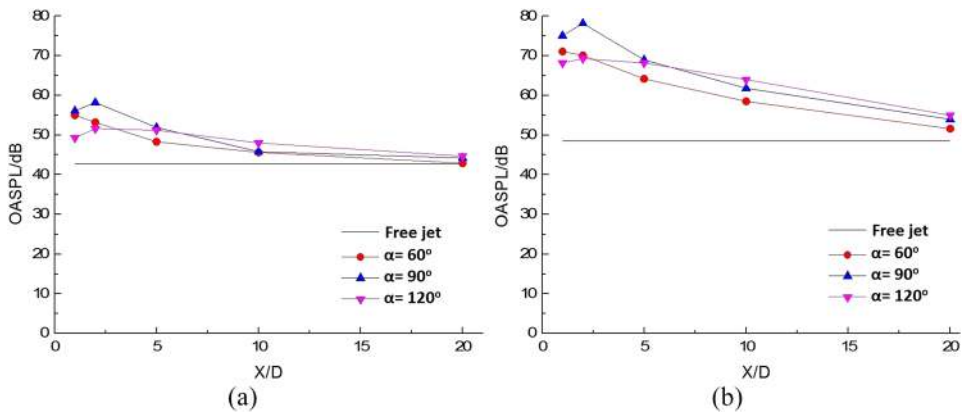

FIG. 8. Variation of OASPL with impinging distance for different cone angles (θ=45°). (a) Impinging velocity of 30m/s. (b) Impinging velocity of 60m/s.

As the impinging distance increases to 20D, the OASPL of impinging jet is approaching to that of the free jet.

In summary, as the impinging distance changes, the cone angle has different effects on variation of OASPL. The following spectral analysis shows cone angle effects on the source characteristics with different impinging distances.

C. Spectrum analysis

Fig. 9 shows the one-third octave spectrum of impinging jet for different cone angles at various impinging distances. The impinging velocity is 60m/s and the θ value of 45° is chosen for the presentation. It can be observed that the SPL variation of the free jet has the low

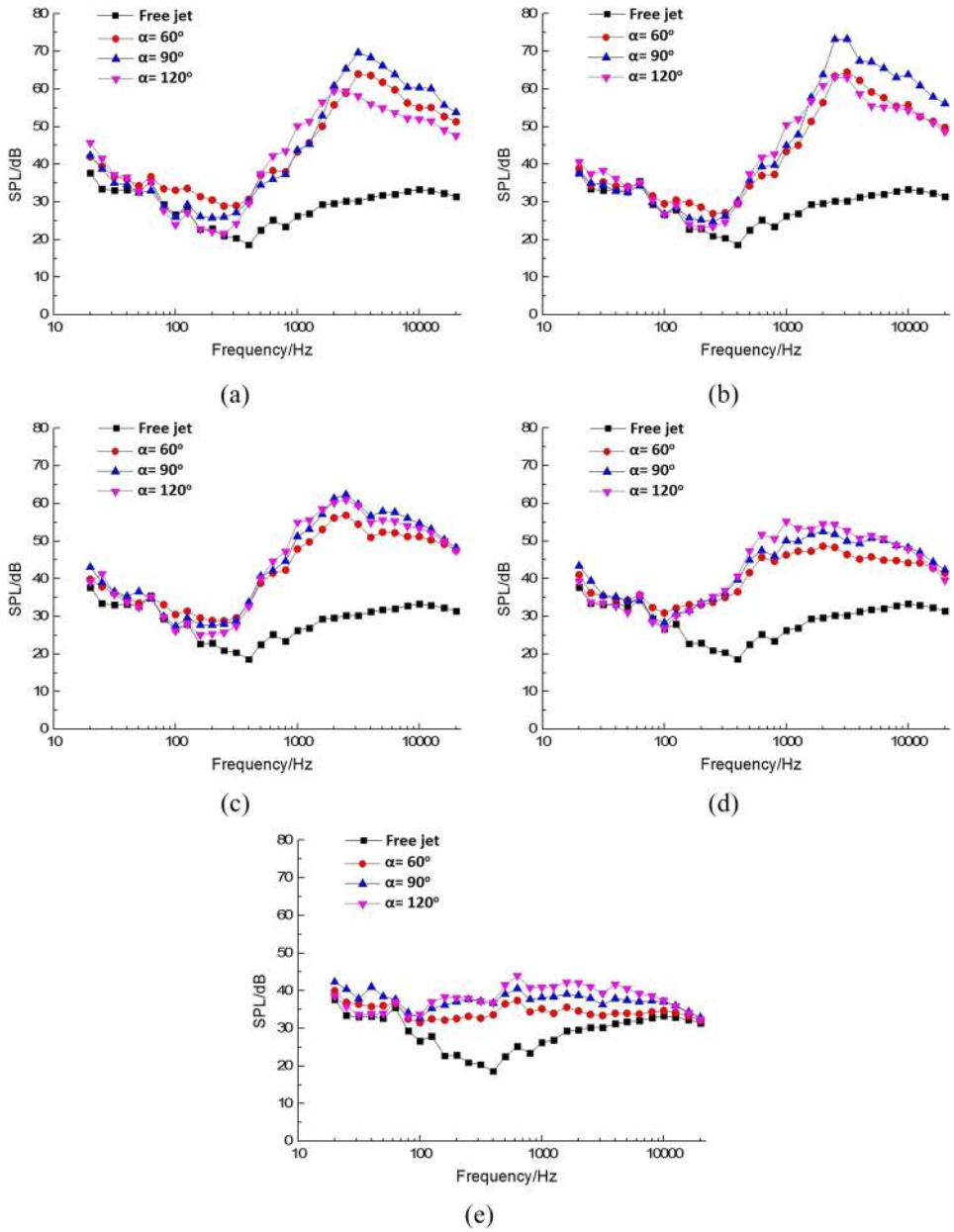

FIG. 9. One-third octave spectrum of impinging jet for different cone angles at various impinging distances (θ=45°). (a) X=1D. (b) X=2D. (c) X=5D. (d) X=10D. (e) X=20D.

frequency characteristic and the SPL decreases first and then increases with the increase of frequency. The minimum value occurs at 400Hz center band. Compared with the free jet case, the main difference of impinging jet cases is the higher SPL in the middle and high frequency bands. When the cone is close to the nozzle outlet (X<5D), the peak noise is present in all cases and the dominant components are identified as a broadband in the range 1600~5000 Hz center bands. As the cone angle increases, the SPL of the dominant components increases first and then decreases.

With the increase of the impinging distance (X>5D), the peak noise is gradually less obvious. The frequency range of the dominant components increases, whereas the SPL decreases in the middle and high frequency bands for all cases. As the cone angle increases, the SPL of the dominant components increases.

Moreover, as the impinging distance increases to 20D, the SPL trend of all cone angle cases is of typical broadband characteristics. Compared with the free jet case, the main difference of the impinging jet cases is the higher SPL in the middle frequency bands of 200~2000Hz.

D. Acoustic source analysis

Combined with flow field analysis and noise characteristic analysis, main acoustic sources of impinging jet with different cone angles and impinging distances are investigated. For the free jet case, the main acoustic source is the quadrupole source caused by the internal stress of the fluid with low-frequency characteristic. For the impinging jet case, the main acoustic source is of broadband characteristic and generated by the coupling of three factors: internal stress of the fluid, pressure fluctuation on the surface of the cone and vortices shedding from the cone. When the obstacle is close to the nozzle (like X=1D), the length of potential core area decreases sharply. The intensity of the quadrupole source is weaken. The main acoustic source is the dipole source with broadband characteristic in the middle and high frequency band, which is caused by the pressure fluctuation and the vortex-shedding. As the cone angle increases, the intensity of vortex-shedding decreases, whereas the length of wall jet region increases. From acute angle to right angle, the intensity increase of pressure fluctuation has a more important effect on the source than the intensity reduction of vortex-shedding. However, from right angle to obtuse angle, the intensity reduction of vortex-shedding plays a more important role. It leads to the OASPL increasing first and then decreasing.

With the increase of impinging distance, the intensity of the quadrupole source increases and the intensity of the pressure fluctuation and the vortex-shedding is reduced. According to the spectrum analysis, the intensity reduction of vortex-shedding plays a more important role on the intensity decrease of the dipole source. The conclusion can be consistent with the fact that the OASPL increases with the increase of the cone angle.

When the obstacle is far from the nozzle (like X=20D), the flow field in the free jet region for the impinging jet cases is similar to that for the free jet case. The main acoustic source is the quadrupole source. The conclusion is in good agreement with the fact that the spectrum for the impinging cases is gradually similar to the spectrum for the free jet case. Cone angle has little effect on the acoustic source.

E. Noise directivity

Noise directivity of the impinging jet for different cone angle cases is investigated to provide theoretical support for noise reduction. Based on A-weighted networks, Fig. 10 shows the OASPL vs θ plots for the free jet case and different cone angle cases with impinging distances X/D=1,5,10, monitoring angles in the range $15° \leqslant \theta \leqslant 165°$, and the impinging velocity of 60m/s. It is observed that the OASPL for impinging jet cases is much larger than that for the free jet case. As the monitoring angle θ increases, the OASPL of the free jet decreases. For X=1D the noise directivity is similar in different cone angle cases. The OASPL decreases first and then increases as θ increases. The maximum OASPL occurs in angles close to 30° and 150°. The minimum OASPL occurs in angles close to 75°.

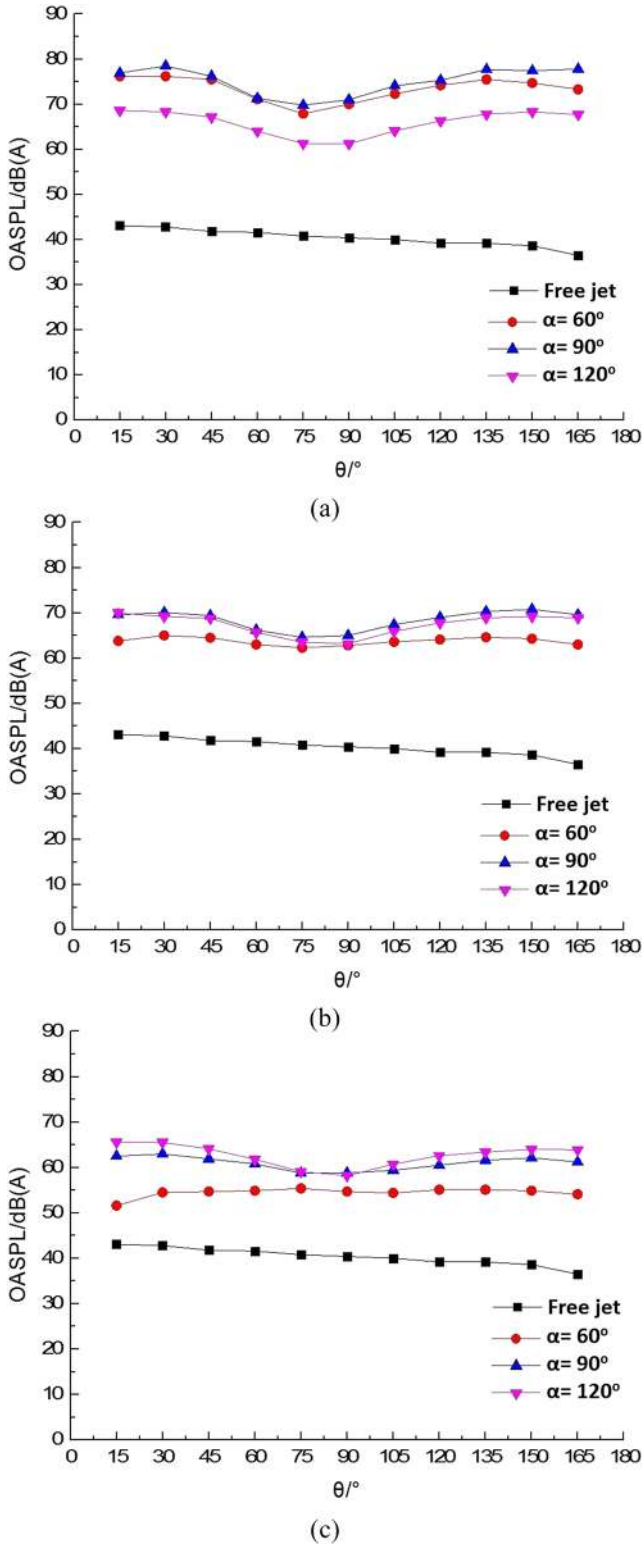

FIG. 10. Noise directivity for different cone angle cases under various impinging distances. (a) X=1D. (b) X=5D. (c) X=10D.

As the impinging distance increases, the cone angle has a great effect on the noise directivity. For α=90° and 120°, the trend of noise distribution is similar. However, as for α=60°, the noise distribution is gradually uniform and the minimum OASPL occurs in angles close to 15°.

IV. CONCLUSIONS

Noise characteristics of impinging jet on the conical obstacle are experimentally investigated by varying parameters such as cone angle (α=60°, 90° and 120°), impinging velocity (from 20m/s to 60m/s) and impinging distance (X/D=1, 2, 5, 10 and 20). Experimental acoustic data are obtained including overall sound pressure level (OASPL) and noise spectrum. Flow field is analyzed using velocity measurement. Acoustic source study is conducted combining with the analysis of flow field and noise characteristics. Noise directivity study is performed to provide theoretical support for noise reduction. The results indicate that effects of cone angle on noise characteristics of the impinging jet are mainly related to the impinging distance. The main noise characteristic for impinging jet cases is of broadband characteristic in the middle and high frequency bands.

When the cone is close to the nozzle, the OASPL value of the impinging jet increases first and then decreases with increase of the cone angle. The main acoustic source is the dipole source generated by vortex-shedding and pressure fluctuation. The noise directivity is similar in different cone angle cases. The OASPL decreases first and then increases as the monitoring angle θ increases. As the impinging distance increases, the effect of cone angle has changed. The OASPL increases with the increase of the cone angle. The intensity of the quadrupole source increases and the intensity of the dipole source is reduced. The intensity reduction of vortex-shedding plays a more important role on the intensity decrease of the dipole source. The trend of noise distribution is similar for α= 90° and 120°. As for α= 60°, the noise distribution is gradually uniform and the minimum OASPL occurs in angles close to 15°.When the cone is far from the nozzle, the main acoustic source is the quadrupole source. The OASPL of impinging jet for all cone angle cases is approaching to that of the free jet.

ACKNOWLEDGMENTS

This work was financially supported by the National Natural Science Foundation of China (No.51376077).

[1] A. Abdel-Fattah, "Numerical and experimental study of turbulent impinging twin-jet flow," Experimental Thermal & Fluid Science **31**(8), 1061–1072 (2007).
[2] A. Dhamanekar and K. Srinivasan, "Effect of impingement surface roughness on the noise from impinging jets," Physics of Fluids **26**(3), 132–143 (2014).
[3] G. Sinibaldi, G. Lacagnina, L. Marino, and G. P. Romano, "Aeroacoustics and aerodynamics of impinging supersonic jets: Analysis of the screech tones," Phys Fluids **25**(8), 393–405 (2013).
[4] D. Arthurs and S. Ziada, "Self-excited oscillations of a high-speed impinging planar jet," Journal of Fluids & Structures **34**(4), 236–258 (2012).
[5] M. Akamine, K. Okamoto, K. L. Gee, T. B. Neilsen, S. Teramoto, T. Okunuki, and S. Tsutsumi, "Effect of nozzle-plate distance on acoustic phenomena from supersonic impinging jet," AIAA J. **56**(5), 1943–1952 (2018).
[6] A. Frendi and M. R. Brown, "Flow structures and noise from a supersonic impinging jet," Int J Numer Method H **26**(8), 1–20 (2016).
[7] G. Romain, B. Christophe, and M. Olivier, "Investigation of tone generation in ideally expanded supersonic planar impinging jets using large-eddy simulation," J Fluid Mech **808**, 90–115 (2017).
[8] B. Christoph, J. A. Housman, and C. C. Kiris, "Noise generation mechanisms for a supersonic jet impinging on an inclined plate," J Fluid Mech **797**, 802–850 (2016).
[9] A. Lyrintzis, V. Golubev, K. Kurbatski, E. Osman, and R. Mankbadi, "Detached-eddy simulations of rocket plume noise at lift-off," J Acoust Soc Am **136**(4), 2168 (2014).
[10] Z. Yao, H. Liu, and X. Zhang, "Interaction of shocks and vortices in a highly underexpanded supersonic impinging jet," AIAA J. **50**(5), 1169–1176 (2012).
[11] A. Uzun, R. Kumar, M. Y. Hussaini, and F. S. Alvi, "Simulation of tonal noise generation by supersonic impinging jets," AIAA J. **51**(7), 1593–1611 (2013).
[12] T. Nonomura, H. Honda, Y. Nagata, M. Yamamoto, S. Morizawa, S. Obayashi, and K. Fujii, "Plate-angle effects on acoustic waves from supersonic jets impinging on inclined plates," AIAA J. **54**(3), 1–12 (2015).
[13] S. I. Kim and S. O. Park, "Oscillatory behavior of supersonic impinging jet flows," Shock Waves **14**(4), 259–272 (2005).
[14] A. Powell, "On the edgetone," J Acoust Soc Am **33**(4) (1961).
[15] A. Powell, "Nature of the sound sources in low—Speed jet impingement—Further considerations," J Acoust Soc Am **90**(6), 3326–3331 (1991).
[16] B. R. Vinoth and E. Rathakrishnan, "Effect of impinging plate geometry on the self-excitation of subsonic impinging jets," Journal of Fluids & Structures **27**(8), 1238–1251 (2011).
[17] H. Ren, G. Zhang, and H. Guan, "Three-dimensional numerical simulation of a vortex ring impinging on a circular cylinder," Fluid Dyn Res **47**(2) (2015).

[18] R. Vinze, S. Chandel, M. D. Limaye, and S. V. Prabhu, "Influence of jet temperature and nozzle shape on the heat transfer distribution between a smooth plate and impinging air jets," Int J Therm Sci **99**, 136–151 (2016).
[19] F. Afroz and M. R. Sharif, "Numerical study of turbulent annular impinging jet flow and heat transfer from a flat surface," Appl Therm Eng **138** (2018).
[20] A. Hadipour and M. R. Zargarabadi, "Heat transfer and flow characteristics of impinging jet on a concave surface at small nozzle to surface distances," Appl Therm Eng **138** (2018).